ACS APPLIED MATERIALS & INTERFACES

RESEARCH ARTICLE

www.acsami.org

Load-Induced Transitions in the Lubricity of Adsorbed Poly(L-lysine)-*g*-dextran as a Function of Polysaccharide Chain Density

Kenneth J. Rosenberg,[†,‡] Tolga Goren,[†] Rowena Crockett,[§] and Nicholas D. Spencer*[,†]

[†]Laboratory for Surface Science and Technology, Department of Materials, ETH Zurich, Wolfgang-Pauli-Strasse 10, CH-8093 Zurich, Switzerland

[§]Empa, Swiss Federal Institute for Materials Science and Technology, Ueberlandstrasse 129, CH-8600 Duebendorf, Switzerland

Supporting Information

ABSTRACT: Chain-density gradients of poly(L-lysine)-*graft*-dextran (PLL-*g*-dex), a synthetic comblike copolymer with a poly(L-lysine) backbone grafted with dextran side chains, were fabricated on an oxidized silicon substrate. The influence of the changing dextran chain density along the gradient on the local coefficient of friction was investigated via colloidal-probe lateral force microscopy. Both in composition and structure, PLL-*g*-dex shares many similarities with bottlebrush biomolecules present in natural lubricating systems, while having the advantage of being well-characterized in terms of both architecture and adsorption behavior on negatively charged oxide surfaces. The results indicate that the transition of the dextran chain density from the mushroom into the brush regime coincides with a sharp reduction in friction at low loads. Above a critical load, the friction increases by more than an order of magnitude, likely signaling a pressure-induced change in the brush conformation at the contact area and a corresponding change in the mechanism of sliding. The onset of this higher-friction regime is moved to higher loads as the chain density of the film is increased. While in the low-load (and low-friction) regime, increased chain density leads to lower friction, in the high-load (high-friction) regime, increased chain density was found to lead to higher friction.

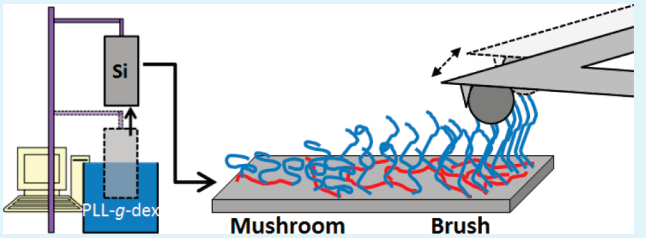

KEYWORDS: aqueous lubrication, boundary lubrication, friction, surface-chemical gradients, molecular architecture

INTRODUCTION

The molecular architecture and structure of bottle-brush polymers such as poly(L-lysine)-*graft*-poly(ethylene glycol) (PLL-*g*-PEG), and their use in modifying surface properties, have been the subject of several recent studies.[1−5] In particular, these polymers are attractive friction-reduction additives in an aqueous environment, because they tend to adsorb onto surfaces to form dense brushlike layers, in which the highly solvated nature of the extending polymer chain is known to correlate well with effective lubrication.[3,4,6−8] Recently, the lubrication properties of poly(L-lysine)-*graft*-dextran (PLL-*g*-dex) with a variety of grafting ratios and dextran molecular weights under aqueous conditions were also studied both on the macro- and the nanoscale.[9,10] It was shown that PLL-*g*-dex lubricates metal oxide surfaces very efficiently, and readily forms high-density polymer brush layers with properties dependent on the molecular weight of the dextran side chains.

Dextran is a naturally occurring polysaccharide consisting of an α(1→6)-linked glucan with branches attached to the 3-positions of the straight-chain glucose units. PLL-*g*-dex is formed by grafting dextran chains onto the backbone of poly(L-lysine), a polycation that spontaneously adsorbs onto negatively charged surfaces, such as metal oxides, at multiple points via the ungrafted, primary amine groups, as shown in Figure 1. The resulting graft copolymer, PLL-*g*-dex, is highly soluble in water, and, when bound to a substrate at sufficient density, effectively renders the surface nonfouling, similarly to other dextran-containing surfaces.[9,11−15] The overall stability of PLL-*g*-dex, similar to that of PLL-*g*-PEG, is a

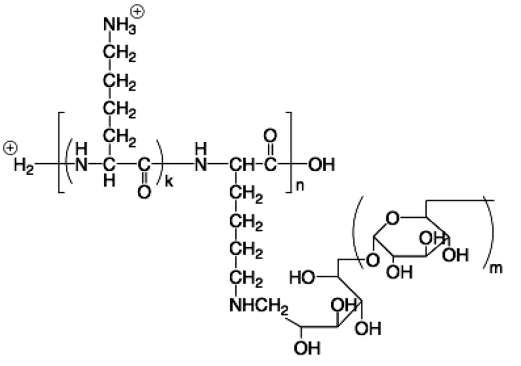

Figure 1. Structure of PLL-*g*-dextran copolymer with grafting ratio $k + 1$.

Received: April 28, 2011
Accepted: July 12, 2011
Published: July 12, 2011

feature that biomedical applications can readily exploit, for example as a gene-delivery vector.[16,17] In contrast to PEG, however, dextran is not prone to undesirable oxidation reactions and possesses multiple reactive sites, enabling further functionalization and chemical modification.

An important characteristic of PLL-*g*-dex that it shares with virtually all lubricious biomolecules is the presence of oligosaccharide side chains. Many studies have focused on the lubricating properties of glycoproteins, including lubricin and naturally occurring polysaccharides on a variety of substrates and under various environmental conditions.[18] Low friction and wear are normally associated with the complex mixtures that constitute natural lubricious layers, which often consist of highly hydrated glycoproteins, such as proteoglycans and mucins.[18] A common difficulty in interpreting these measurements lies in the complexity of the structure and composition of the glycoproteins. The topological complexity of the molecules, and the subtle differences in the electrostatic and hydrophobic interactions that govern the adsorption properties, lead to an uncertainty in adsorbed conformation. This presents a challenge when attempting to determine the features contributing to lubricity. In PLL-*g*-dex, the composition and structure are much simpler than in glycoproteins, and thus it constitutes a biomimetic system that maintains the critical features important for lubricity.

In the present study, we examine the relationship between the density of dextran chains and the frictional properties of the resulting system. Although a great deal is known regarding the structure of polymer films and their interactions, much less is understood regarding how changes in polymer conformation and, as a consequence, film mechanical properties, influence friction.[19−21] The conformation of surface-attached polymer chains is dependent on the mean spacing between neighboring chains L and the radius of gyration, R_g. When $L \gg 2R_g$, the non-overlapping, isolated chains are restricted in conformation only by the surface, and may assume a pancake- or mushroom-shaped conformation, depending on the interaction of the polymer with the surface. At the other extreme, for $L<2R_g$ (the brush regime), the interchain steric repulsive interactions cause the chains to assume more extended conformations. The use of a gradient to generate gradual changes in polymer chain density is convenient for producing the full range of conformations. Gradients, in general, are a powerful technique in studying parametric dependency, as evidenced by their use in a variety of applications, including wetting[22,23] and cell-adhesion[24] studies. For example, using a grafting-density gradient of poly(acrylamide) (PAAm) on silica, Genzer and co-workers measured the mushroom-to-brush transition point (0.065 chains/nm^2), based on height measurements obtained by ellipsometry, and correlated variations in chain density with wetting properties.[25]

MATERIALS AND METHODS

Poly(L-lysine)-graft-dextran (PLL-*g*-dex). The PLL-*g*-dex copolymer used in these experiments was synthesized as described previously.[9,10] Briefly, dextran (dextran T5, 5.2 kDa, polydispersity 1.8, Pharmacosmos A/S, Denmark) undergoes reductive amination with poly(L-lysine)-HBr (20 kDa, polydispersity 1.1, Sigma-Aldrich, Switzerland). The solvent for the reaction was a sodium borate buffer (0.1 M, pH 8.5, 0.4 M NaCl). The terminal dextran aldehyde group was first reacted with the primary amine groups of PLL to form a Schiff base, which was subsequently reduced by sodium cyanoborohydride ($NaBH_3CN$). The resultant PLL-*g*-dex graft copolymer was separated from the unreacted materials through filtration with ultracentrifugation. The specific ratio of lysine monomers to dextran chains is defined as the grafting ratio and can be controlled during synthesis by adjusting the reactant ratio.[26,27] The grafting ratio was determined through ^{1}H-NMR spectroscopy of PLL-*g*-dex in D_2O and elemental analysis (EA).

The particular copolymer studied here was PLL(20)-*g*[5.3]-dex(5), where 20 kDa is the molar mass of PLL including the Br^- counterions, 5.3 is the grafting ratio, and 5 kDa is the weight-average molecular weight (M_w) of the dextran. On average, dex(5) consists of 32 monomer units, which assuming each monomer is 0.7 nm long corresponds to a fully stretched chain length of 22 nm.

Gradient Preparation. Bare silicon wafers of 2 cm × 1 cm were cleaned by sonicating twice in toluene, then twice in 2-propanol, each for five minutes. Next, the substrates were exposed to O_2 plasma for two minutes (Plasma Cleaner/Sterilizer, PDC-32G instrument, Harrick, Ossining, NY, USA). The thickness of the surface SiO_2 layer was measured by ellipsometry (described below), after which each substrate was immediately dipped at a controlled rate into a 0.02 mg/mL solution of PLL-*g*-dex in 1 mM 4-(2-hydroxyethyl)-1-piperazineethanesulfonic acid (HEPES) at pH 7.4.[28] After removal from the PLL-*g*-dex HEPES solution, the substrate was first rinsed with polymer-free HEPES buffer to remove any weakly bound or nonadsorbed PLL-*g*-dex, and then copiously rinsed with ultrapure water (Milli-Q Gradient A10, Millipore SA, Molsheim, France) and finally dried under N_2. The final PLL-*g*-dex thicknesses were then measured in 2 mm increments along the substrate by ellipsometry.

Both SiO_2 and PLL-*g*-dex film thicknesses were measured in ambient air by ellipsometry using a M-2000 V spectroscopic ellipsometer (J.A. Woollam Co., Inc., Lincoln, NE, USA) at 65°, 70°, and 75° at wavelengths between 370-1000 nm. The variable-angle spectroscopic ellipsometry (VASE) spectra were analyzed using WVASE32 software. The "dry" thickness of PLL-*g*-dex was obtained by fitting the VASE spectra to a multilayer model based on the optical properties of a generalized Cauchy layer (A = 1.45, B = 0.01, C = 0).[29] The results of ellipsometric characterization of a PLL-*g*-dex surface-chemical gradient are shown in Figure 2A. The dry thickness of the copolymer layer ranges from below the experimental scatter of SiO_2 thickness (0.1 Å) at the bare end to 16 ± 1 Å, corresponding to the maximum thickness for this particular PLL-*g*-dex architecture.

The adsorbed mass of PLL-*g*-dex onto a standard $Si_{0.75}Ti_{0.25}O_2$ waveguide in buffer solution was measured via optical waveguide lightmode spectroscopy (OWLS), an optical biosensing technique which monitors the grating-assisted in-coupling of a He−Ne laser into the planar waveguide. Total internal reflection guides the light to the end of the waveguiding layer, where it is detected by a photodiode. The critical angle of reflection is related to the change in refractive index near the waveguide surface upon adsorption of molecules. From this information, and the refractive index increment (dn/dc), the mass and refractive index of the adsorbed layer are calculated[30−32] by the software. The refractive index increment of PLL-*g*-dex was taken to be 0.131.[9]

Prior to the adsorption experiment, the optical waveguide chip (standard: $Si_{0.75}Ti_{0.25}O_2$ on glass, Microvacuum, Budapest, Hungary) was cleaned by ultrasonication in 0.1 M HCl for 10 min, rinsed with ultrapure water, ultrasonicated in 2-propanol for 10 min, rinsed again with ultrapure water, dried under nitrogen, and cleaned in a UV/ozone cleaner (UV/Clean, model 135500, Boeckel industries Inc., Feasterville, PA) for 30 min. The cleaned waveguide was placed into the OWLS flow cell and equilibrated by exposing to HEPES buffer solution overnight, in order to obtain a stable baseline. The waveguide was then exposed to a polymer solution (0.015 mg/mL in a similar HEPES buffer) under constant flow for at least 30 min, resulting in the formation of a polymer adlayer.

Atomic Force Microscope Measurements. The AFM experiments were conducted in contact mode using a Dimension 3000 AFM (Nanoscope III controller, Digital Instruments, Santa Barbara, CA, USA) and a MFP-3D AFM (Asylum Research, Santa Barbara, CA, USA). The probes were commercially available V-shaped Si_3N_4 cantilevers (NP-S20, nominal normal spring constant 0.58 N/m, Veeco,

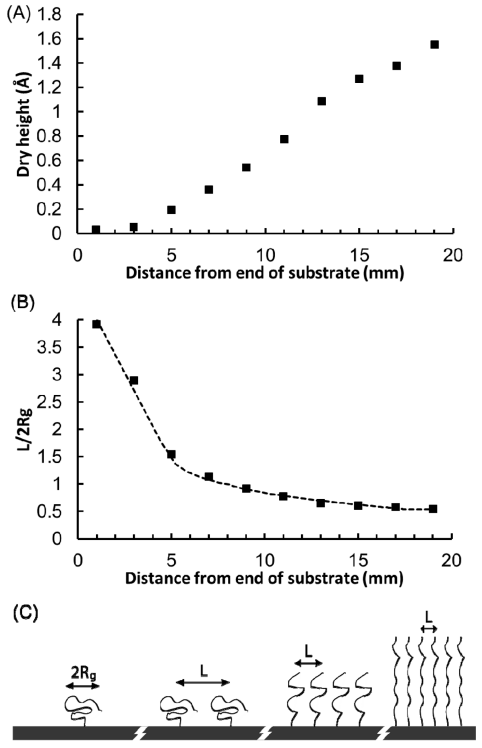

Figure 2. (A) "Dry" height of PLL-*g*-dex along a SiO_2 substrate measured using ellipsometry. (B) Plot of $L/2R_g$ along the gradient obtained by calculating the mean spacing between dextran chains. The dashed line is not a fit of the data, but rather is calculated directly from relating the PLL-*g*-dex adsorption time to adsorbed mass using OWLS data. (C) The resulting chemical gradient consists of isolated dextran chains at one end ($L \gg 2R_g$) and a fully stretched "brush" regime at the opposite end ($L < 2R_g$).

Plainview, NY, USA) and rectangular Si cantilevers (CSC12A, nominal normal spring constant 0.95 N/m, Mikromasch, Tallinn, Estonia).

A borosilicate colloidal sphere (Kromasil®, Eka Chemicals AB, Bohus, Sweden; radius $\approx 3\ \mu$m) was glued to the end of the cantilever with UV-curable epoxy (Norland Optical Adhesive #61 or #63, Norland, Cranbury, NJ, USA). The entire assembly was then irradiated with UV light for 30 min and allowed to sit for at least 1 day to further strengthen the adhesion between the colloidal sphere and the cantilever. The nanotribological experiments described here include measurements taken first with a bare, uncoated SiO_2 colloid probe and then with a PLL-*g*-dex brush-like layer attached to the same colloidal sphere by the same method as used for the gradient preparation, and with sufficiently long exposure to solution to ensure maximum possible brush density (according to the gradient and OWLS kinetics measurements).

Friction measurements were obtained by scanning the probe perpendicularly to the major axis of the cantilever and recording the TMR (Trace Minus Retrace in mV) value. The TMR value is directly proportional to the friction force and minimizes the contributions to the lateral force from non-friction sources.[33] Each bare colloid was first slid against the uncoated part of the gradient until the coefficient of friction reached a constant value. This "running in" step was done to check the quality of the tip and to ensure that any transient colloidal wear or damage could not affect the measured friction. To test for any such changes as well as material transfer from the PLL-*g*-dex gradient, the bare surface was scanned intermittently to ensure the friction response remained constant. Additionally, the gradient was measured in a non-sequential order to minimize possible effects arising from drifting of force sensitivity. All scanning distances were 1 μm with velocities of 1 μm/sec, unless otherwise noted. The dependence of scanning distance on lateral force was investigated and showed that for lengths over 100 nm, the lateral force remained constant.

The normal and lateral forces were calibrated as described in the Supporting Information. Briefly, the cantilever spring constants were calibrated from the power spectral density of the thermal noise fluctuations[34] and by the method of Sader and coworkers.[35] The lateral force measurements of the rectangular cantilevers were calibrated using the test probe method described by Carpick and coworkers,[36] and the measurements of the V-shaped cantilevers were scaled to the resulting curve. Rectangular cantilevers were chosen that approached the normal spring constant of the V-shaped cantilevers while minimizing errors due to in-plane bending.[37]

Following the nanotribological measurements with an uncoated SiO_2 colloid, the entire tip-cantilever assembly was gently lifted off the gradient surface and immediately exposed to a 0.02 mg/mL PLL-*g*-dex solution in 1 mM HEPES to form a brush layer on the colloid, as predicted both by the OWLS and ellipsometry measurements. After 30 minutes, the AFM cantilever was thoroughly rinsed with polymer-free HEPES buffer and placed back into contact with the same gradient substrate to resume the friction experiments.

RESULTS

Measurement of $L/2R_g$. In order to understand how lubrication varies with dextran chain density and conformation, the parameter $L/2R_g$ is calculated along the gradient. Depending on the specific technique used, literature values of R_g of 5 kDa dextran range from 1.9 nm (dynamic light scattering)[38] to 2.4 nm (fluorescence correlation spectroscopy).[39] Because the focus of this study is on the relative, rather than absolute, change in $L/2R_g$, the value of R_g throughout this paper is simply fixed at 1.9 nm. The only effect of setting R_g to 2.4 nm would be to shift all $L/2R_g$ values by about 25% in the direction of lower chain density. Two independent methods to measure L are discussed here. First, from the "dry" PLL-*g*-dex thickness h (Figure 2A), the grafting density of dextran chains $\sigma \approx 1/L^2$ can be found from $\sigma = h\rho N_A/M_N$, where ρ is the bulk polymer mass density, N_A is Avogadro's number, and M_N is the polymer molecular weight.[40] Previous adsorption results of PLL-*g*-dex on SiO_2 substrates measured with optical waveguide lightmode spectroscopy (OWLS) give the maximum amount of adsorbed PLL-*g*-dex as 290 ± 16 ng/cm^2.[9,10] Finally, because h is proportional to $\sigma = 1/L^2$ from the above relationship, L can be calculated at each point along the gradient where h is known. These data points are shown in Figure 2B. Although one end of the substrate was not exposed to PLL-*g*-dex solution, L remains finite because of the experimental uncertainty in the ellipsometric measurement, as mentioned in Materials and Methods.

A separate technique to calculate L utilizes the kinetic adsorption data obtained from OWLS data to map the time exposed to PLL-*g*-dex solution directly to adsorbed polymer mass. In this method, there is no assumption in relating dextran chain density to "dry" thickness. Instead, the adsorption time is known for each position along the gradient, which is then mapped to the OWLS adsorption curve to generate PLL-*g*-dex mass as a function of position. The data from this method is shown as a dashed line in Figure 2B, in excellent agreement with the analytical model described above.

Friction Measurements. Figure 3 shows three representative "friction-load" curves measured with a bare, uncoated SiO_2 colloid probe at different values of $L/2R_g$ along a PLL-*g*-dex gradient. The friction-load curves measured with a coated SiO_2

sphere show a similar shape to those in Figure 3 (not shown). The lateral force (F_L) increases as a function of normal force (F_N) and initially displays linear behavior, as seen in the figure inset. However, upon increasing the load past a critical value, the linear relationship ceases to be valid as the friction, $\mu = dF_L/dF_N$, rapidly increases for each of the curves shown. Continued ramping up of load again results in a constant, but higher, friction value. This transition was not found to occur when the bare silica colloid was sliding against a bare silicon wafer, which yielded a stable friction coefficient of 0.22 across the entire load range, in excellent agreement with literature.[41] The coefficients of friction of both regimes (termed "low load" and "high load") were recorded along the gradient, i.e., at different values of $L/2R_g$, and are shown in Figure 4. The initial slope (low load) for both uncoated and coated colloid is displayed in Figure 4A while both slopes (low and high load) are shown in Figure 4B. Although the coated colloid exhibits a lower friction coefficient at low load, it gives a much higher friction coefficient than the uncoated colloid at high load. The transition in normal load between the low and high friction regimes, defined as F_T, is shown in Figure 5.

DISCUSSION

Effect of $L/2R_g$. Polymer-brush layers at a tribological interface are known to cause a significant reduction in the friction coefficient.[2−4,42] Essentially, the long-range steric interaction arising from the osmotic repulsion at high chain density provides a suitable boundary film to reduce, if not eliminate entirely, direct contact of opposing surfaces.[43] Therefore, it is not surprising that, over the moderate pressures generally studied (in the megapascal range or lower), the lower the value of $L/2R_g$, or, equivalently, the higher the dextran chain density, the lower the coefficient of friction. For $L > 2R_g$, the coefficient of friction is large and relatively independent of dextran density. In this non-brush regime, the rather inhomogeneous distribution of dextran chains along the surface is an ineffective barrier against the external load. In contrast, when $L < 2R_g$, the higher density produces a more homogeneous brush layer that can give rise to a greater steric repulsion. With increasing dextran density, the thickness of the film layer is expected to grow, allowing for greater physical separation for a given load between sliding surfaces. Moreover, as a result of the increasing density of dextran chains, the total amount of associated water within the layer also increases.[9,10] These combined factors of increased physical separation and increased film hydration are instrumental in rapidly lowering the coefficient of friction as the chain density transitions along the gradient from the bare end until the maximum brush density. However, even sub-optimal coverage still functions as an effective barrier layer between the colloid and bare substrate, as evidenced by the roughly twofold friction reduction near $L \sim 2R_g$. This reduction in friction, even at partial coverage, is consistent with other published results indicating that modifying the interfacial properties of solid substrates with adsorbed polymers, not necessarily in the brush regime, still achieves improved lubricity.[44−47]

For identical values of $L/2R_g$, the friction coefficient with the brush-coated colloid is decreased with respect to the uncoated colloid at low loads (Figure 4A). Furthermore, it is apparent that the friction coefficient is highly dependent on the interfacial properties of the sliding and stationary surfaces individually. Specifically, with the uncoated SiO_2 colloid sliding against the uncompressed brush, the friction is much lower than when the brush-coated SiO_2 colloid is sliding against a nearly bare (i.e., very high $L/2R_g$) surface, when both are at low load. Here, even though both systems consist of similar surfaces within the

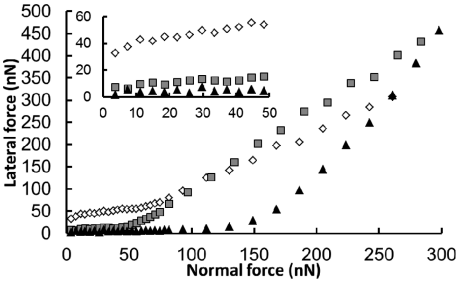

Figure 3. Set of typical friction vs. load curves of a bare SiO_2 colloidal probe sliding on a PLL-*g*-dex-coated SiO_2 gradient for $L/2R_g = 2.9$ (◇), $L/2R_g = 1.2$ (■), and $L/2R_g = 0.6$ (▲). The inset zooms in on the data obtained up to $F_L = 50$ nN.

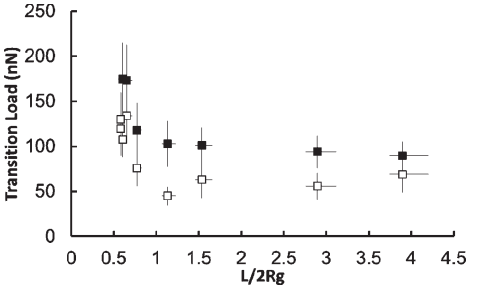

Figure 5. Characteristic load at which the friction starts to deviate from linearity, denoted as the transition load, is shown as a function of $L/2R_g$ along the gradient with uncoated colloid sphere (open) and PLL-*g*-dex-coated colloid sphere (filled).

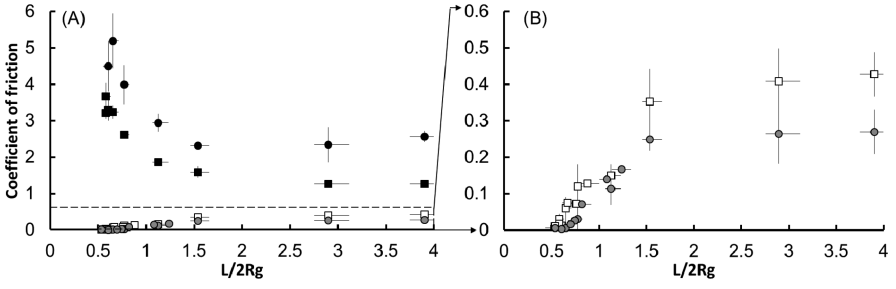

Figure 4. Coefficient of friction plotted against $L/2R_g$ (A) in both low and high load ($F_L > 100$ nN) and (B) just low load ($F_L < 50$ nN) regimes. The squares represent a bare SiO_2 colloid at low load (empty) and high load (filled). The circles represent a PLL-*g*-dex-coated SiO_2 colloid at low load (grey) and high load (black).

tribocontact, the surface histories are very different. Presumably the continual shearing of the brush-coated colloid against the relatively bare substrate has a wearing effect on the brush, in comparison with the uncoated colloid sliding across the uncompressed, previously unperturbed brush.

Effect of Load. The tribological response of the PLL-*g*-dex gradient to external load exhibits two distinct linear regimes over the loading range studied (Figure 3) At low loads, the lateral force increases linearly up to a transition load F_T (Figure 3 inset), after which it increases with a higher slope. From Figure 5, the value of F_T measured along the gradient with an uncoated SiO_2 colloidal sphere remains virtually constant as $L/2R_g$ is decreased, with a value around 60 nN, until $L/2R_g$ reaches unity, F_T nearly doubling by $L/2R_g = 0.6$. The similarity between the dependence of F_T and friction coefficient on $L/2R_g$ is most likely not coincidental—that is, the stiffer and more hydrated PLL-*g*-dex caused by the more densely packed dextran chains leads to both a decrease in friction and an increase in F_T. As expected, with the brush attached to the colloid, the ability of the polymer film within the tribocontact to support an external load is increased compared with a bare colloid. In other words, the presence of the brushlike layer on the sliding colloid helps to maintain a lower friction coefficient before the friction abruptly rises, above F_T. For both the coated and uncoated colloidal sphere, as the dextran chain density on the gradient increases towards full brush, F_T rises in response to the growing steric repulsion of the PLL-*g*-dex layer.

Interestingly, although this transition in the friction—load curve has been observed in a variety of polymer brush systems, both neutral and charged,[48] the literature provides no answers as to a possible mechanism. A similar transition in friction with increasing brush compression, caused by increasing load, has also been predicted for entangled polymer brush systems,[21] in contrast to nonentangled systems. Although the dextran chains studied are likely too short and stiff to experience entanglement, their interchain hydrogen bonding can have a comparable effect. The transition load represents the tipping point of an energy balance between brush compression and brush parting or interpenetration, for the bare and brush-coated colloidal spheres, respectively. If interchain hydrogen bonds, which scale with brush density, are assumed to behave comparably to rapidly forming entanglements, they serve as a hindrance to this transition by resisting the parting of the brush. Additionally, the friction of the brush-on-brush system at high loads may be particularly exacerbated by the formation and disruption of new hydrogen bonds between the chains of the interpenetrating brushes. A simplified Hertzian analysis shows that the contact pressures in the 'low' regime are still far higher than those commonly achieved in physiological conditions.[49] For $F_L \approx 10$ nN, with a colloid radius of ~3.5 μm, the maximum pressure reaches ~50 MPa. For comparison, the typical contact pressures seen in joints are normally only 10% of this value, and many lubricated physiological tribosystems have far lower contact pressures (e.g., in the eye).

CONCLUSIONS

The lubricating properties of a density gradient of PLL-*g*-dex copolymer were investigated by means of colloidal-probe lateral force microscopy. The dominant parameter determining the coefficient of friction was the relative spacing ($L/2R_g$) of the surface-grafted dextran chains. Furthermore, the nanotribological analysis showed that the friction coefficient along the gradient is highly load dependent. At high contact loads, the lubrication behavior is very different compared to that at low loads, both for brush-brush and brush-surface contact. Although higher polysaccharide chain densities lower friction more effectively at low loads, they actually increase friction in the high-load regime compared to lower chain densities.

Although this study highlights potential design limits in the use of polysaccharide brushes, it also opens new potential toward high-friction applications of polymer coatings. Although this study only examined the effect of dextran chain density, other architectural parameters may be critical in determining the overall friction, including grafting ratio and dextran molecular weight. These initial studies should prove useful in better designing and tuning PLL-*g*-dex and related copolymers for specific water-based lubrication systems.

ASSOCIATED CONTENT

Supporting Information. Description of the specific instruments and procedures used to obtain lateral force measurements, and the method by which the normal and lateral forces were calibrated. This material is available free of charge via the Internet at http://pubs.acs.org.

AUTHOR INFORMATION

Corresponding Author
*E-mail: nspencer@ethz.ch.

Present Addresses
‡Merck, WP75B-210, West Point, PA, 19486, USA.

ACKNOWLEDGMENT

The authors are grateful for financial support by the Swiss National Science Foundation.

REFERENCES

(1) Lee, S. W.; Spencer, N. D. In *Superlubricity*; Erdemir, A., Martin, J.-M., Eds.; Elsevier Science B.V.: Amsterdam, 2007; Chapter 21.
(2) Pasche, S.; De Paul, S. M.; Vörös, J.; Spencer, N. D.; Textor, M. *Langmuir* **2003**, *19*, 9216–9225.
(3) Lee, S.; Müller, M.; Ratoi-Salagean, M.; Vörös, J.; Pasche, S.; De Paul, S. M.; Spikes, H. A.; Textor, M.; Spencer, N. D. *Tribol. Lett.* **2003**, *15*, 231–239.
(4) Müller, M.; Lee, S.; Spikes, H. A.; Spencer, N. D. *Tribol. Lett.* **2003**, *15*, 395–405.
(5) Yan, X. P.; Perry, S. S.; Spencer, N. D.; Pasche, S.; De Paul, S. M.; Textor, M.; Lim, M. S. *Langmuir* **2004**, *20*, 423–428.
(6) Lee, S.; Iten, R.; Müller, M.; Spencer, N. D. *Macromolecules* **2004**, *37*, 8349–8356.
(7) Kobayashi, M.; Terayama, Y.; Hosaka, N.; Kaido, M.; Suzuki, A.; Yamada, N.; Torikai, N.; Ishihara, K.; Takahara, A. *Soft Matter* **2007**, *3*, 740–746.
(8) Chen, M.; Briscoe, W. H.; Armes, S. P.; Klein, J. *Science* **2009**, *323*, 1698–1701.
(9) Perrino, C.; Lee, S.; Choi, S. W.; Maruyama, A.; Spencer, N. D. *Langmuir* **2008**, *24*, 8850–8856.
(10) Perrino, C.; Lee, S.; Spencer, N. D. *Tribol. Lett.* **2009**, *33*, 83–96.
(11) Massia, S. P.; Stark, J. *J. Biomed. Mater. Res., Part A* **2001**, *56*, 390–399.
(12) Martwiset, S.; Koh, A. E.; Chen, W. *Langmuir* **2006**, *22*, 8192–8196.
(13) Piehler, J.; Brecht, A.; Hehl, K.; Gauglitz, G. *Colloids Surf., B* **1999**, *13*, 325–336.

(14) Holland, N. B.; Qiu, Y. X.; Ruegsegger, M.; Marchant, R. E. *Nature* **1998**, *392*, 799–801.
(15) Frazier, R. A.; Matthijs, G.; Davies, M. C.; Roberts, C. J.; Schacht, E.; Tendler, S. J. B. *Biomaterials* **2000**, *21*, 957–966.
(16) Ferdous, A.; Watanabe, H.; Akaike, T.; Maruyama, A. *Nucleic Acids Res.* **1998**, *26*, 3949–3954.
(17) Maruyama, A.; Watanabe, H.; Ferdous, A.; Katoh, M.; Ishihara, T.; Akaike, T. *Bioconjugate Chem.* **1998**, *9*, 292–299.
(18) Lee, S.; Spencer, N. D. *Science* **2008**, *319*, 575–576.
(19) Perry, S. S.; Yan, X.; Yan, X.; Limpoco, F. T.; Lee, S.; Müller, M.; Spencer, N. D. *ACS Appl. Mater. Interfaces* **2009**, *1*, 1224–1230.
(20) Grest, G. S. *Phys. Rev. Lett.* **1996**, *76*, 4979–4982.
(21) Goujon, F.; Malfreyt, P.; Tildesley, D. J. *Macromolecules* **2009**, *42*, 4310–4318.
(22) Chaudhury, M. K.; Whitesides, G. M. *Science* **1992**, *256*, 1539–1541.
(23) Genzer, J. *J. Adhes.* **2005**, *81*, 417–435.
(24) Singh, N.; Cui, X. F.; Boland, T.; Husson, S. M. *Biomaterials* **2007**, *28*, 763–771.
(25) Wu, T.; Efimenko, K.; Vlcek, P.; Subr, V.; Genzer, J. *Macromolecules* **2003**, *36*, 2448–2453.
(26) Lane, C. F. *Synthesis* **1975**, 135–146.
(27) Borch, R. F.; Bernstein, M. D.; Durst, H. D. *J. Am. Chem. Soc.* **1971**, *93*, 2897–2904.
(28) Morgenthaler, S.; Zink, C.; Stadler, B.; Vörös, J.; Lee, S.; Spencer, N. D.; Tosatti, S. G. P. *Biointerphases* **2006**, *1*, 156–165.
(29) Feller, L. M.; Cerritelli, S.; Textor, M.; Hubbell, J. A.; Tosatti, S. G. P. *Macromolecules* **2005**, *38*, 10503–10510.
(30) Höök, F.; Vörös, J.; Rodahl, M.; Kurrat, R.; Böni, P.; Ramsden, J. J.; Textor, M.; Spencer, N. D.; Tengvall, P.; Gold, J.; Kasemo, B. *Colloids Surf., B* **2002**, *24*, 155–170.
(31) Vörös, J.; Ramsden, J. J.; Csucs, G.; Szendrö, I.; Textor, M.; Spencer, N. D. *Biomaterials* **2002**, *23*, 3699–3710.
(32) Kurrat, R.; Textor, M.; Ramsden, J. J.; Böni, P.; Spencer, N. D. *Rev. Sci. Instrum.* **1997**, *68*, 2172–2176.
(33) Ruan, J.-A.; Bhushan, B. *J. Mater. Res.* **1993**, *8*, 3019–3022.
(34) Cook, S. M.; Schaffer, T.E.; Chynoweth, K.M.; Wigton, M.; Simmonds, R.W.; Lang, K.M. *Nanotechnology* **2006**, *17*, 2135–2145.
(35) Sader, J. E.; Chon, J. W. M.; Mulvaney, P. *Rev. Sci. Instrum.* **1999**, *70*, 3967–3970.
(36) Cannara, R. J.; Eglin, M.; Carpick, R. W. *Rev. Sci. Instrum.* **2006**, *77*, 053701–11.
(37) Sader, J. E.; Green, C. P. *Rev. Sci. Instrum.* **2004**, *75*, 878–884.
(38) Malvern Zetasizer Nano application note MRK839-01, 2007.
(39) Görisch, S. M.; Wachsmuth, M.; Tóth, K. F.; Lichter, P.; Rippe, K. *J. Cell Sci.* **2005**, *118*, 5825–5834.
(40) Wu, T.; Gong, P.; Szleifer, I.; Vlcek, P.; Subr, V.; Genzer, J. *Macromolecules* **2007**, *40*, 8756–8764.
(41) Vaarelski, I. U.; Brown, S. C.; Rabinovich, Y. I.; Moudgil, B. M. *Langmuir* **2004**, *20*, 1724–1731.
(42) Pettersson, T.; Naderi, A.; Makuska, R.; Claesson, P. M. *Langmuir* **2008**, *24*, 3336–3347.
(43) Yamamoto, S.; Ejaz, M.; Tsujii, Y.; Fukuda, T. *Macromolecules* **2000**, *33*, 5608–5612.
(44) Zou, Y.; Rossi, N. A. A.; Kizhakkedathu, J. N.; Brooks, D. E. *Macromolecules* **2009**, *42*, 4817–4828.
(45) Klein, J.; Kumacheva, E.; Mahalu, D.; Perahia, D.; Fetters, L. J. *Nature* **1994**, *370*, 634–636.
(46) Kampf, N.; Gohy, J. F.; Jerome, R.; Klein, J. *J. Polym. Sci., Part B: Polym. Phys.* **2005**, *43*, 193–204.
(47) Raviv, U.; Giasson, S.; Kampf, N.; Gohy, J. F.; Jerome, R.; Klein, J. *Nature* **2003**, *425*, 163–165.
(48) Liberelle, B.; Giasson, S. *Langmuir* **2008**, *24*, 1550–1559.
(49) Benz, M.; Chen, N. H.; Jay, G.; Israelachvili, J. I. *Ann. Biomed. Eng.* **2005**, *33*, 39–51.